



Invited Paper

Frenkel-exciton Hamiltonian for dendrimeric nanostar

Tatsuya Minami, Sergei Tretiak, Vladimir Chernyak, Shaul Mukamel*

Department of Chemistry, University of Rochester and Rochester Theory Centre for Optical Science and Engineering,
P.O. RC Box 270216, Rochester, NY 14627-0216, USA

Abstract

Exciton energies and transfer matrix-elements for the nanostar (a perylene chromophore attached to a polyphenylacetylene dendrimer) are obtained by computing the linear absorption of several segments using the collective electronic oscillator (CEO) approach. Our results allow a first-principles calculation of an effective Frenkel exciton Hamiltonian which can describe the optical properties as well as energy transfer and funneling in this artificial antenna complex. © 2000 Elsevier Science B.V. All rights reserved.

Keywords: Frenkel exciton model; Phenylacetylene dendrimer; Nanostar; Collective electron oscillator method

A new class of macromolecules with dendrimeric (tree-like) geometry has been suggested as possible candidates for artificial antenna systems [1–4]. The combination of the large number of absorbing units at the molecular periphery and the downhill energy gradient of the electronic states towards the center makes it possible to harvest the light effectively and transfer energy to a reaction center or a chemical sensor attached to the center [4–7]. Shortreed et al. [8] had measured the absorption and the fluorescence spectra of the nanostar dendrimer shown in Fig. 1 and found efficient exciton funneling from the periphery to the chemical sensor (perylene) located at the core of the antenna.

Recent experimental [7] and theoretical [9] investigations clearly show that the optical excitations of polyphenylacetylene (PPA) dendrimers are localized within the linear segments and involve no charge-transfer-type excitations. This suggests that the Frenkel exciton model [10] should be applicable for computing the optical response. Using this model, Poliakov et al. [11] had investigated various optical and electronic features of compact dendrimers, composed of identical diphenylacetylene linear segments connected by meta substitutions of the benzene rings. Meta branching

disrupts the charge transfer (electron–hole separation) between segments and the compact dendrimers can be modeled as an assembly of two-level (ground and excited state) chromophores with Coulomb interaction responsible for excitation transfer. The excitation energy of linear segments and exciton hopping matrix elements were computed using the collective electronic oscillator (CEO) procedure [9,12]. To simulate the funneling effect reported in Ref. [8], in this article, we extend the exciton model of Ref. [11] to the nanostar dendrimer shown in Fig. 1.

The Frenkel exciton Hamiltonian reads [10]

$$H \equiv \sum_m \Omega_m B_m^\dagger B_m + \sum_{m,n}^{m \neq n} J_{mn} B_m^\dagger B_n - \mathbf{P} \cdot \mathcal{E}(t), \quad (1)$$

$$\mathbf{P} \equiv \sum_m \boldsymbol{\mu}_m (B_m^\dagger + B_m). \quad (2)$$

Here the indices m and n label linear PPA segments of the dendrimer tree. B_m^\dagger (B_m) are creation (annihilation) operators of an electron–hole pair (exciton) on the m th segment. Ω_m and $\boldsymbol{\mu}_m$ are the corresponding excitation energy and transition dipole moment, respectively. $\mathcal{E}(t)$ is the external optical field and J_{mn} represent the exciton transfer matrix elements, i.e. the electrostatic interaction between n th and m th segments. Since J_{mn} decreases rapidly with the n to m distance, we only retain nearest-neighbor couplings (i.e. between linear segments connected by a benzene ring at the meta position).

* Corresponding author. Fax: + 1-716-473-6889.

E-mail address: mukamel@chem.rochester.edu (S. Mukamel)

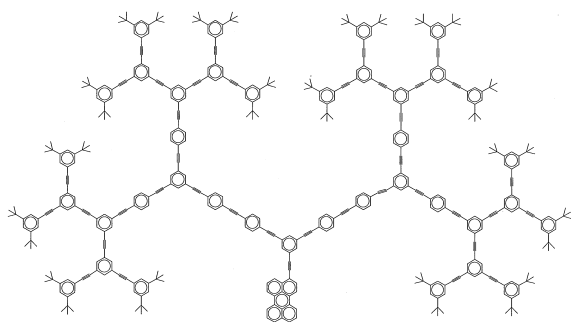


Fig. 1. Structure of the nanostar dendrimer [7].

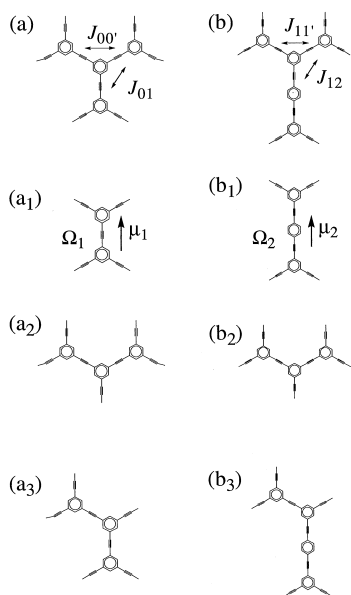


Fig. 2. (a) and (b) Trimers used for geometry optimization; (a₁) and (b₁) monomer segments used for determining Ω_1, μ_1 , and Ω_2, μ_2 ; (a₂) and (b₂) dimer segments used for determining $J_{00'}$ and $J_{11'}$; (a₃) and (b₃) dimer segments used for determining J_{01} and J_{12} .

The nanostar has four different types of linear segments. We label the segments as follows: The first, second and third generation segments will be labeled 3, 2, and 1, respectively (denoting the number of triple bonds in each segment). The central segment with the perylene will be labeled 4. Finally, the fourth (one triple bond) generation will be labeled 0 [see (a₁) and (b₁) in Fig. 2, as well as (c₁) and (d₁) in Fig. 3]. Two segments belonging to the same generation and sharing a common benzene ring will be distinguished by a prime (1 and 1', etc). Using this notation the nanostar has four exciton energies $\Omega_1 \dots \Omega_4$, four "intra-generation" $J_{00'}$, $J_{11'}$, $J_{22'}$ and $J_{33'}$, and four "inter-generation" J_{01} , J_{12} , J_{23} and J_{34} exciton

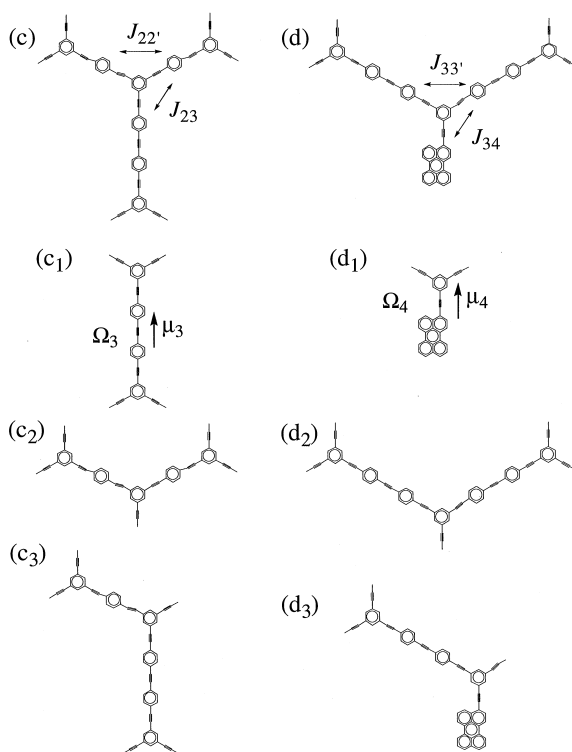


Fig. 3. (c) and (d) Trimers used for geometry optimization; (c₁) and (d₁) monomer segments used for determining Ω_3, μ_3 , and Ω_4, μ_4 ; (c₂) and (d₂) dimer segments used for determining $J_{22'}$ and $J_{33'}$; (c₃) and (d₃) dimer segments used for determining J_{23} and J_{34} .

transfer parameters [see (a) and (b) in Fig. 2, and (c) and (d) in Fig. 3]. In addition there are four transition dipole moments $\mu_1 \dots \mu_4$ [note that $\Omega_0 = \Omega_1$ and $\mu_0 = \mu_1$]. As shown in Ref. [11], we can assume that the transition dipole moment on each segment is directed along the triple bond and points from the center to the periphery [see (a₁) and (b₁) in Fig. 2, as well as (c₁) in Fig. 3]. The direction of the transition dipole moment on the perylene chromophore at the center is also shown in (d₁) of Fig. 3.

The Frenkel–Hamiltonian parameters [Eq. (1)] of the nanostar [Fig. 1] Ω_m, J_{mn} and μ_m were obtained using the semi-empirical CEO quantum chemistry algorithms [9,12,13]. We follow the procedure of Ref. [11] as outlined below. We first consider trimers (a) and (b) in Fig. 2 as well as (c) and (d) in Fig. 3. Geometries of these trimers were optimized at the AM1 level using Gaussian 98.

Ω_m and μ_m are the excitation energy and transition dipole moment of the lowest absorption peak of the molecule representing the corresponding linear segment. To obtain these parameters we picked out the monomer segments (a₁) and (b₁) in Fig. 2 as well as (c₁) and (d₁) in Fig. 3, retaining the trimer geometry. We then calculated

the linear absorption for these monomers by the CEO approach and obtained $\Omega_1 \dots \Omega_4$ as the peak position of the absorption, and $\mu_1 \dots \mu_4$ as the transition dipole moment of these states.

We next turn to the calculation of intra-generation transfer. To that end we consider the dimer segments (a_2), (b_2), (c_2) and (d_2) obtained from our four trimers, again retaining the trimer geometry. CEO calculation of the linear absorption of each dimer yields $\Delta\varepsilon$ as the energy splitting of the two peaks. The transition dipoles of the various absorption peaks are obtained as well, and used to determine the sign of the various J coupling matrix elements. We then considered the solution of the Frenkel exciton Hamiltonian for these dimers. Let us discuss (a_2) of Fig. 2 as an example. Its eigenvalue problem reads

$$\begin{pmatrix} \Omega_1 & J_{11'} \\ J_{11'} & \Omega_1 \end{pmatrix} \begin{pmatrix} \varphi_\alpha(1) \\ \varphi_\alpha(2) \end{pmatrix} = \varepsilon_\alpha \begin{pmatrix} \varphi_\alpha(1) \\ \varphi_\alpha(2) \end{pmatrix}, \quad (\alpha = 1,2). \quad (3)$$

From the solution of this equation, we obtain the excitonic energies ε_1 , ε_2 and coupling $|J_{11'}| = \Delta\varepsilon/2 = |\varepsilon_1 - \varepsilon_2|/2$, where $\Delta\varepsilon$ is the energy splitting between two electronic states. The excitonic energies are computed by the CEO procedure: the linear absorption calculation of the dimer results in two low-frequency absorption peaks with energies ε_1 and ε_2 .

To determine the sign of $J_{11'}$, we consider the oscillator strength of these two excited states labeled by α in Eq. (3). The transition dipole moments for each linear segment are

$$\boldsymbol{\mu}(1) = \mu_1 \begin{pmatrix} -\sin \pi/3 \\ \cos \pi/3 \end{pmatrix}, \quad \boldsymbol{\mu}(2) = \mu_2 \begin{pmatrix} \sin \pi/3 \\ \cos \pi/3 \end{pmatrix} \quad (4)$$

and the corresponding oscillator strengths are

$$f_\alpha = |\boldsymbol{\mu}(1)\varphi_\alpha(1) + \boldsymbol{\mu}(2)\varphi_\alpha(2)|^2. \quad (5)$$

The oscillator strengths depend on the sign of $J_{11'}$. We thus fix the sign to make f_α consistent with the CEO linear absorption spectrum.

To compute the inter-generation transfer parameters, we examined the dimers (a_3), (b_3), (c_3) and (d_3) obtained from the trimers without changing the geometry. We then consider the solution of the Frenkel exciton Hamiltonian for these dimers. For example (b_3) in Fig. 2, eigenvalue problem reads

$$\begin{pmatrix} \Omega_1 & J_{12} \\ J_{21} & \Omega_2 \end{pmatrix} \begin{pmatrix} \varphi_\alpha(1) \\ \varphi_\alpha(2) \end{pmatrix} = \varepsilon_\alpha \begin{pmatrix} \varphi_\alpha(1) \\ \varphi_\alpha(2) \end{pmatrix}, \quad (\alpha = 1,2). \quad (6)$$

By solving the equation, we obtain $|J_{12}| = \frac{1}{2}\sqrt{\Delta\varepsilon^2 - \Delta\Omega^2}$ where $\Delta\Omega \equiv |\Omega_1 - \Omega_2|$. $\Delta\varepsilon$ is obtained from the linear absorption of the dimer calculated by the CEO approach, whereas Ω_1 and Ω_2 are monomeric excitation energies. To determine the sign of J_{12} , we again considered the oscillator strengths for the

Table 1

Excitation energies Ω , exciton transfer J parameters and transition dipole moments μ of the Frenkel Hamiltonian. Ω and J are in cm^{-1} , μ are normalized relative to μ_1

Ω_1	Ω_2	Ω_3	Ω_4
29044	26347	25058	21011
$J_{00'}$	$J_{11'}$	$J_{22'}$	$J_{33'}$
-69	-72	347	326
J_{01}	J_{12}	J_{23}	J_{34}
69	-158	-325	-302
μ_1	μ_2	μ_3	μ_4
1.00	1.67	2.06	1.47

two excited states. The transition dipole moment for each linear segment reads

$$\boldsymbol{\mu}(1) = \mu_1 \begin{pmatrix} -\sin \pi/3 \\ \cos \pi/3 \end{pmatrix}, \quad \boldsymbol{\mu}(2) = \mu_2 \begin{pmatrix} 0 \\ 1 \end{pmatrix}. \quad (7)$$

As in the previous case, we choose the sign of J_{12} to make the oscillator strength agree with the CEO calculation of the spectrum.

The complete set of Ω , J and μ parameters which define the Frenkel exciton Hamiltonian [Eq. (1)] obtained by this procedure are given in Table 1.

Using these exciton parameters, we have computed the linear absorption spectrum [11]

$$\sigma(\omega) \equiv \sum_\alpha \frac{2|\boldsymbol{\mu}_\alpha|^2 \Gamma}{(\omega - \varepsilon_\alpha)^2 + \Gamma^2}. \quad (8)$$

Here ε_α denote the eigenvalues of the Frenkel exciton Hamiltonian [Eq. (1)] without the external field, with the corresponding eigenfunctions

$$|\varphi_\alpha\rangle \equiv \sum_m \varphi_\alpha(m) B_m^\dagger |0\rangle. \quad (9)$$

$\boldsymbol{\mu}_\alpha$ is the transition dipole moment of the α th exciton,

$$\boldsymbol{\mu}_\alpha \equiv \sum_m \boldsymbol{\mu}_m \varphi_\alpha(m). \quad (10)$$

Γ is the exciton dephasing rate. The calculation displayed in Fig. 4 properly represents all the experimental features [7]. In this figure the calculated spectrum was shifted by 33 nm to the blue region. The present results make it possible to carry out a first-principles numerical simulation of the time- and frequency-gated fluorescence [14] which should provide a direct probe for exciton transport. The relative efficiency of various antennae could then be systematically compared.

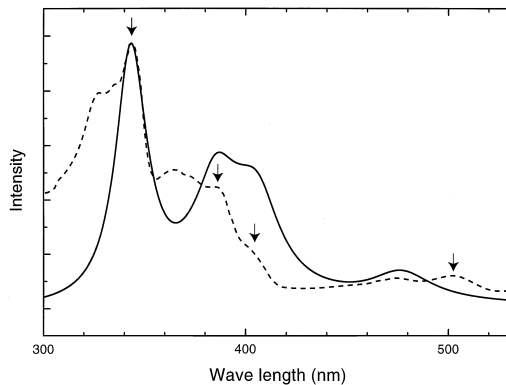


Fig. 4. Solid line calculated absorption spectrum of the nanostar with the parameters of Table 1 and $\Gamma = 806 \text{ cm}^{-1}$; dashed line experimental spectrum [7]. The arrows indicate the zero-phonon absorption peaks. The calculated spectrum was shifted to the blue by 33 nm to make the highest peak coincide with experiment.

Acknowledgements

The support of the National Science Foundation and the Air Force Office of Scientific Research is gratefully acknowledged.

References

- [1] D.L. Jiang, T. Aida, *Nature* 388 (1997) 454.
- [2] M. Enomoto, T. Aida, *J. Am. Chem. Soc.* 121 (1999) 874.
- [3] S. Jockusch, J. Ramirez, K. Sanghvi, R. Nociti, N.J. Turro, D.A. Tomalia, *Macromolecules* 32 (1999) 4419.
- [4] C. Devadoss, P. Bharathi J.S. Moore, *J. Am. Chem. Soc.* 118 (1996) 9635.
- [5] Z.-Y. Shi, W. Tan, Z. Xu, J. Moore, R. Kopelman, *J. Lumin.* 76&77 (1998) 193.
- [6] M. Shortreed, Z.-Y. Shi, R. Kopelman, *Mol. Cryst. Liq. Cryst.* 28 (1996) 95.
- [7] R. Kopelman, M. Shortreed, Z.-Y. Shi, W. Tan, Z. Xu, J. Moore, A. Bar-Haim, J. Klafter, *Phys. Rev. Lett.* 78 (1997) 1239.
- [8] M.R. Shortreed, S.F. Swallen, Z.-Y. Shi, W. Tan, Z. Xu, C. Devadoss, J.S. Moore, R. Kopelman, *J. Phys. Chem. B* 101 (1997) 6318.
- [9] S. Tretiak, V. Chernyak, S. Mukamel, *J. Am. Chem. Soc.* 119 (1997) 11408.
- [10] E.A. Silinich, V. Capek, *Organic Molecular Crystals*, American Institute of Physics, New York, 1994.
- [11] E.Y. Poliakov, V. Chernyak, S. Tretiak, S. Mukamel, *J. Chem. Phys.* 110 (1999) 8161.
- [12] S. Mukamel, S. Tretiak, T. Wagersreiter, V. Chernyak, *Science* 277 (1997) 781.
- [13] S. Tretiak, V. Chernyak, S. Mukamel, *J. Phys. Chem. B* 102 (1998) 3310.
- [14] V. Chernyak, T. Minami, S. Mukamel, *J. Chem. Phys.*, submitted.